scientific reports

Check for updates

OPEN

A reduction in effective population size has not relaxed purifying selection in the human population of Eivissa (Balearic Islands)

Julen Aizpurua-Iraola[1], Elisa Marí-Cardona[2], Maria Barber-Olives[3], David Comas[1] & Francesc Calafell[1]✉

Ibiza (Eivissa) is one of the main Balearic Islands in the western Mediterranean. Recent studies have highlighted the genetic distinctiveness of present-day Eivissans within the region and suggested it could be attributed to the genetic drift caused by recent demographic events. Whether this distinctiveness emerged from a differential demographic history, or rather from a bias for sampling in a small geographic region such as Eivissa, remains an open question, together with the understanding of the functional consequences of demography in the island. In order to clarify these questions and further characterize the distinctiveness of Eivissa within the Balearic and Mediterranean context, we generated whole exome sequences for 31 and 20 individuals from Eivissa and Menorca respectively, a subset of which were also genotyped with the Human Origins array. Our results show that Eivissans present signs of putatively recent genetic isolation that are shared to a lesser extent with Menorca such as more and longer runs of homozygosity and high numbers of intra-population shared IBD segments. Regarding the functional consequences of recent demography, although Eivissans do not present an excess of deleterious alleles or homozygotes comparing to other populations, genetic drift seems to have increased the allele frequencies of neutral and deleterious variants, which can have various medical implications.

Keywords Human population genetic, Demography, Balearic Islands, Whole exome sequences, Mutation load.

Ibiza (Eivissa) and Menorca are, together with Mallorca and Formentera, the main islands in the Balearic Archipelago in the Western Mediterranean. Despite having similar sizes and geographic characteristics, Eivissa and Menorca have been the scenario of slightly different human histories. The archipelago was first colonized in the 3rd millennia BCE by people from the Iberian Peninsula[1,2]. During prehistory, although it is true that Mallorca and Menorca have been more thoroughly studied, Eivissa and Formentera (known as the Pityusic islands) present a modest archeological record in comparison, exemplified by the near absence[3] of the cyclopean fortified buildings that characterize the Bronze and Iron Age pre-Talaiotic and Talaiotic periods in Mallorca and Menorca[4]. This absence suggests the Pityusic Islands held a smaller population during prehistory. However, around the beginning of the last millennium BCE, Phoenicians stablished a settlement at the Bay of Eivissa around 654 BCE which would then give rise to the Phoenician city of Ibusim or Ebusus (nowadays Eivissa city), one of the most important commercial spots in the Western Mediterranean, which came with a considerable demographic growth in the island[5]. During the Phoenician, and later, the Punic (Carthaginian) control periods, Eivissa was the main trade hub in the Balearic Islands and one of the most important in the Western Mediterranean. With the Roman invasion of the Balearic Islands after the Punic wars, all the territory passed to Roman rule, which, with the years, diluted the importance of Eivissa[6]. After the Roman and the shorter Vandal and Byzantine rule periods, the Islamic Umayyad Caliphate ruled the Iberian Peninsula and the Balearic Islands for around half a millennium. By this time, the relevance of Eivissa in the Mediterranean was probably limited, as suggested by the scarce archeological record during the 7th and 8th centuries CE[7].

[1]Departament de Medicina i Ciències de la Vida, Institut de Biologia Evolutiva (CSIC-UPF), Universitat Pompeu Fabra, Dr. Aiguader 88, Barcelona 08003, Catalonia, Spain. [2]Departament de Medicina i Ciències de la Vida (MELIS), Universitat Pompeu Fabra, Barcelona, Spain. [3]Clinical Trials Office, Institut d'Oncologia Vall d'Hebron (VHIO), Barcelona, Spain. ✉email: francesc.calafell@upf.edu

In 1231, the Aragonese crown invaded Mallorca that was then under the Almohad Caliphate rule, as the different Christian kingdoms conquered Muslim territories southwards in the 'Reconquista' of the Iberian Peninsula. Eivissa was conquered in the year 1235, while the rulers of Menorca signed a vassalage pact with King James I of Aragon that prevented the island to become part of Aragon, until 1287, when Alphonse III conquered Menorca. Demographically, this was a significant event in the Balearic Islands since the islands were repopulated after most previous inhabitants abandoned the islands or were enslaved[8]. The repopulation was incentivized by the Aragonese crown who granted economic privileges to new settlers coming mainly from present-day Catalonia[9].

Although Eivissa flourished economically during antiquity, Menorca surpassed it partly due to its natural ports, which attracted the interest of different European colonial empires such as the British, who ruled over Menorca for 71 years during the 18th century[8]. On the contrary, after the Catalan colonization, Eivissa underwent relative isolation that might have been caused by the decline in the number of large land estates, resulting in impoverishment of rural areas which developed a subsistence economy based on agriculture. However, this process did not occur in Mallorca and Menorca[10,11].

From a genetic standpoint, the distinctiveness of Eivissa was already suggested in uniparental marker studies due to a possible genetic continuity from Phoenician times[12,13]. More recent studies confirmed Eivissa as a genetic isolate and rejected the Phoenician contribution by comparing present-day individuals with (i) an ancient Phoenician from Eivissa, and (ii) modern Levantines[14,15]. Instead, they suggested that their genetic distinctiveness was the result of isolation and drift, as reflected in their Runs of Homozygosity (ROH) patterns and diversity statistics. These patterns were not detected in a small number of samples from Mallorca and Menorca, which might be evidence for a different demographic history in Eivissa.

Islands tend to be geographically isolated and have limited population sizes, making them prone to the effects of genetic drift, sometimes involving founder effects, and therefore they are more likely to harbor genetic population isolates[16]. Population isolates are known to exhibit different hallmark features of genetic variation, such as lower levels of genetic diversity, larger and increased number of ROHs and regions of the genome identical by descent (IBD) shared within the population, a characteristic variant distribution with fewer segregating sites but higher allele frequencies in those sites segregating[17–22], and finally, an accumulation of deleterious variants and deleterious homozygotes as a result of an efficiency loss in purifying selection, a concept referred to as mutation load[23]. In the past few years, different studies have studied the impact of recent demography on human genomes, and although most of its consequences (ROHs, IBDs, allele frequency shifts, among others) are well known, the extent to which mutation load is affected has been under debate. Studies that analyzed whether Out-of-Africa populations showed an increased mutation load compared to sub-Saharan populations found that, despite substantial shifts in the overall frequency spectrum, the efficiency of purifying selection was not affected leaving no traces of increased mutation load[24,25]. On the other hand, other studies addressed these questions on populations that underwent more recent bottlenecks followed by small effective population sizes and isolation. Their results showed that these populations present signs of isolation, together with an increase of the recessive mutation load interpreted as a relaxation of purifying selection (Casals et al., 2013; Lucas-Sánchez et al., 2021, 2024; Pedersen et al., 2017; Font-Porterias et al., 2021). It is noteworthy that measuring mutation load is not straightforward, and since selection coefficients (i.e. how strongly selection acts to remove an allele) and dominance of all variants are unknown, different statistics have been employed to measure mutation load[23].

Previous results indicate that Eivissa is a genetic isolate in the Western Mediterranean[14], although this might be an artifact of how the samples were obtained, that is, by sampling from individuals from a relatively small territory, which were then compared to larger populations. Moreover, the extent to which the demographic history of Eivissa has affected the functional variation remains unresolved. With this in mind, we present a genomic characterization of the population of Eivissa focusing on the functional variation. Given their different demographic histories, we compare it to the population in Menorca, which has a similar area and population size to Eivissa, as well as with Sardinians, known to be another Mediterranean isolate[26] and to the population of the Iberian Peninsula (IBS), a general population without a history of isolation. We show the genomic consequences of recent demography in Eivissa and Menorca, discussing its historical causes and possible medical implications.

Materials and methods

Samples and sequencing

We collected and sequenced 33 Eivissan and 22 Menorcan samples obtained from healthy unrelated volunteers with the condition of having four of their grandparents born in their respective islands. The participants gave their informed consent after being appropriately informed about the aims of the project. This project was approved by the CEIm-PSMAR IRB in Barcelona (2019/8900/I). All the research in this manuscript has been conducted following the principles outlined in the Declaration of Helsinki.

We captured and sequenced the whole exome of the collected samples with the Agilent SureSelect Human All Exon V6 capture kit, and a subset of the samples (26 for Eivissa and 19 for Menorca) were additionally genotyped with the Affymetrix Human Origins array.

Data processing and quality controls

The fastq files obtained from sequencing were trimmed to remove adaptors with Trimmomatic[27]. Before and after trimming, the quality of the reads was assessed with FastQC[28]. Following the GATK best practices recommendations[29], we mapped the reads to the GRCh38 human reference genome using the Burrows-Wheeler Aligner (BWA) v.0.7.15[30]. The mapped reads were filtered based on their quality (<30) with Samtools[31], the duplicated reads were marked and removed with Picard Tools[32], the indels were realigned with and the quality scores of the reads were recalibrated with GATK IndelRealigner and BaseRecalibrator respectively[29]. Qualimap 2[33] was used to assess the quality of the BAM files at the beginning and after all processing steps (STable 1).

Exome variants were called for the newly genotyped samples together with the samples from reference populations to ensure we obtained a homogeneous final variant set (Fig. 1a). Whole genome sequences (WGS) from the 1000 Genomes Project (1KGP)[34] and the Human Genome Diversity Project (HGDP), together with the whole exome sequence (WES) BAM files from previously published Tunisian Arab samples[19] were remapped to the Homo_sapiens_assembly38 version of the GRCh38 human reference genome downloaded from the GATK resource bundle. GATK HaplotypeCaller was used to produce individual gvcfs, and GenotypeGVCFs was used to jointly genotype them[29]. In addition to the exome variant calling, we also called the genotypes overlapping with the Affymetrix Human Origins (HO) Array for the case of the reference populations collected from the 1KGP and HGDP, which were then merged with the HO array data from the Tunisian Arab samples and the newly genotyped Eivissan and Menorcan samples.

The newly genotyped samples had a mean coverage of 61.3X with an average 5X breadth of coverage of 94.7% on the exome target. After the removal of two low quality samples, these figures increased to 63.2X of mean coverage and a 5X breadth of 96.3% (STable 1).

Samples were filtered according to their mean coverage (keeping samples with > 50X), breadth of coverage (keeping samples with > 95% of the reference at 5X), missingness (excluding samples with > 5% of missing positions) and heterozygosity (excluding samples with > 4 standard deviations over the population average). Two samples were discarded due to their low mean coverage and one sample was filtered out due to an excess of heterozygosity. Variants in non-biallelic sites, not passing the Variant Quality Score Recalibration (VQSR) or mapping to the sexual chromosomes were excluded; the remaining variants were filtered for their coverage (minimum of 5X was required), genotype quality (minimum GQ of 20), missingness (a maximum missingness of 5% was allowed over both WES and WES-Array complete datasets), deviations from Hardy-Weinberg equilibrium (positions with H-W deviations with a p-value $< 10^3$ were excluded) using VCFtools 0.1.16[35] and following the same criteria as in[18–20]. Individual relatedness was assessed using KING v.3[36]: sample pairs with a third-degree relatedness or closer were tagged, and the sample with the lowest mean coverage was excluded from the analysis. Finally, processing and quality checking resulted in two different datasets: a WES dataset with 987,153 SNPs and the following sample counts per population: Eivissa $n = 31$, Menorca $n = 20$, IBS $n = 48$, Sardinia $n = 24$, CEU $n = 50$, TSI $n = 35$, Tunisian Arabs $n = 33$, Palestinian $n = 39$, Mozabite $n = 23$; and a WES-array dataset with 1,288,578 SNPs and the same sample sizes except for Eivissa ($n = 25$) and Menorca ($n = 19$).

As an additional quality check, we counted at the per sample discordances for the overlapping positions between the HO Array data and the exome data. Two samples were excluded from the WES-Array dataset due to their high discordance rate that was compatible with mislabeling (SFigure 1).

Population structure analyses

For PCA and Admixture analyses, both datasets were used after first being pruned for linkage disequilibrium (--indep-pairwise 50 5 0.5) and rare alleles (< 1% minor allele frequency) with PLINK 1.9[37] yielding ~ 144 K and ~ 213 K SNPs for the WES and WES-Array datasets respectively. SmartPCA from the EIGENSOFT software package[38] was used to perform the PCA. Samples detected as outliers by the software were removed from the analysis. For the Admixture analysis, ADMIXTURE v1.3[39] was used in the unsupervised mode testing for ancestral clusters with K values ranging from 2 to 10 with 20 independent iterations with different random seeds for each K. Common modes among the different runs for each K were identified using pong[40]. Cross-validation error was assessed for each run and mean values were calculated to determine the range with minimum error (SFigure 2).

Ancient samples and modelling

We explored possible differences in the ancestral components present in present day Eivissans and Menorcans compared to other populations. For this, we downloaded and used a subset of a panel of different ancient populations from the Allen Ancient DNA resource[41] and merged them with our modern WES + Array dataset, yielding 177 K SNPs after minor allele frequency (1%) and linkage disequilibrium filters (--indep-pairwise 200 20 0.4) with PLINK 1.9. We explored the ancestral components by using Admixtools 2[42] to model our target populations (Eivissa, Menorca, IBS and Sardinians) with a 5-way distal model with Anatolian Neolithic, Yamnaya, western hunter gatherers, Iranian Neolithic and Moroccan late-Neolithic as sources (see STable 2 for details of the model). In order to accept the result of a model p-values > 0.01 were required. Admixtools 2 was also used on the WES + Array data (213,159 SNPs) to calculate f2, f3 and f4 statistics in order to explore patterns of shared genetic drift between Eivissa, Menorca and IBS after excluding the Balearic individuals from the IBS population.

Ancestral allele determination

The ancestral and derived alleles for each position were determined for the WES dataset using the 10 primate EPO (Enredo-Pecan-Ortheus) multialignment from Ensembl Compara 106. Sites with unknown ancestral alleles were removed from all WES analyses except the population structure ones described above, leaving a final SNP count of 874,379.

IBD sharing and effective population size estimation

Beagle 5.3[43] was first used to phase haplotypes in the WES-Array VCF file. Then, IBD segments were detected with Refine-IBD using the default parameters and with a 2 cM IBD segment length detection threshold[44]. Merge-IBD was used to remove gaps between IBD segments that had at most one discordant homozygote and that were < 0.6 cM long[44]. $IBDN_e$ was used to infer the effective population size across time with IBD segments longer than 2 cM and with default parameters[45]. The IBS sample clustering with Eivissans and the Eivissan sample clustering with Menorcans were excluded for the IBD sharing analyses. To further confirm the founder

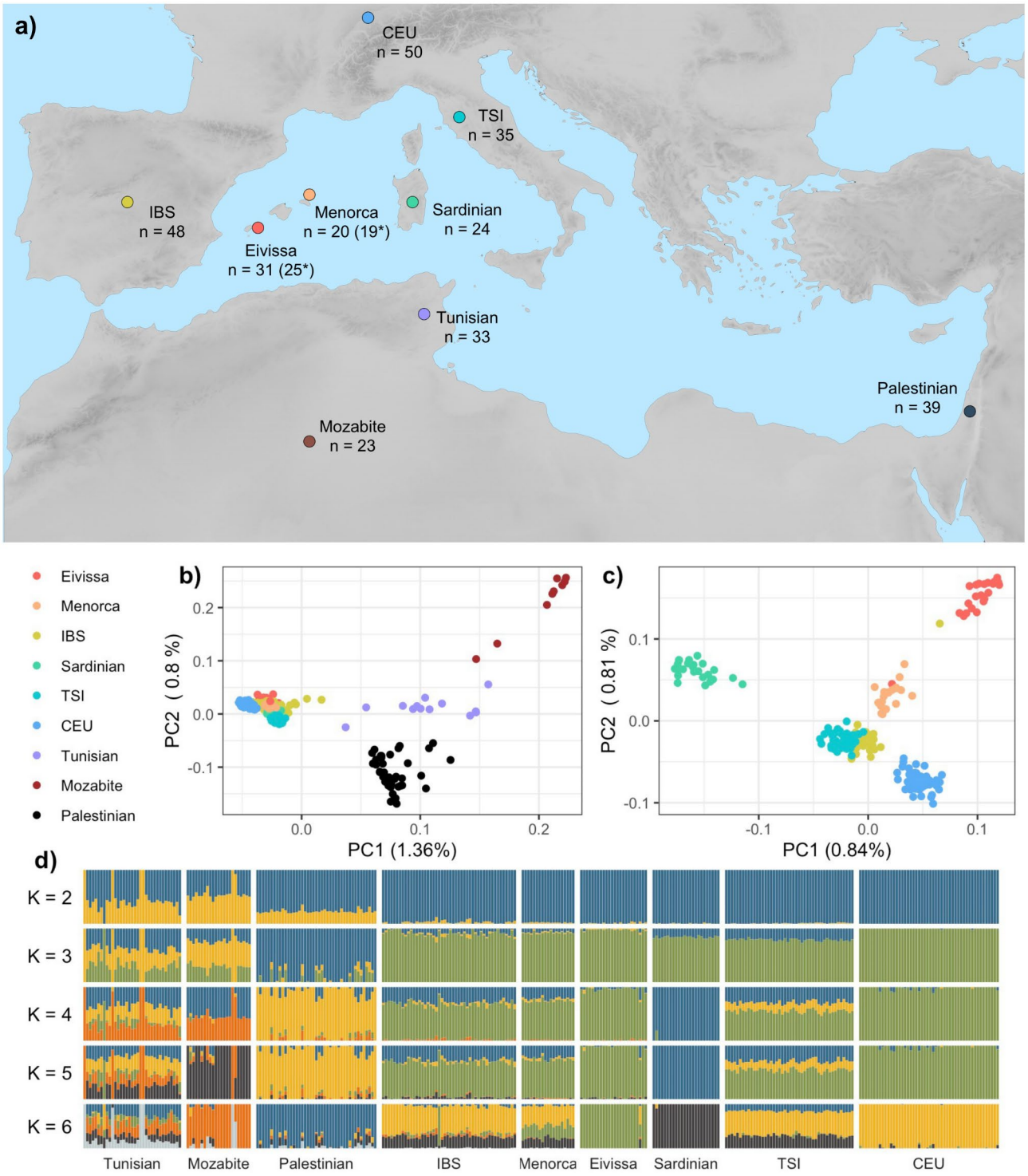

Fig. 1. (**a**) Map of the samples used in the present study with their corresponding sample sizes. Values marked with an asterisk represent the number of samples genotyped with the Human Origins Array. IBS: Iberian from Spain, TSI: Tuscanian from Italy, CEU: Northern-Western Europeans from Utah. The base map was generated in R with the package giscoR with geospatial information obtained from the Geographical information system of the European Commission (GISCO) (which is free to reuse as outlined in https://ec.europa.eu/eurostat/about-us/policies/copyright) and open elevation data obtained from the Open Topography Global Datasets API (https://opentopography.org/developers) with the "elevatr" R package. (**b**) Principal Component Analysis (PCA) of all samples used in the study based on the WES-Array dataset. (**c**) PCA with the European populations in the study. (d) Admixture results from K = 2 to K = 6.

events observed in the $IBDN_e$ analysis, we ran the ASCEND software[46] on the WES-Array dataset with the recommended parameters using Eivissa and Menorca as target populations and IBS as the outgroup population.

Runs of homozygosity (ROHs)

For ROH detection, the WES-Array dataset was first pruned for variants in linkage disequilibrium (--indep-pairwise 50 5 0.8) and then PLINK was used to detect ROHs using sliding windows of 50 SNPs; ROHs were detected if all the 50 SNPs were homozygous. The number of ROHs and total ROH sum were then explored per individual, and finally, we also classified the ROHs by size categories (1-2.5 Mb for short, 2.5-5 Mb for intermediate and > 5 Mb for long ROHs). Differences between populations were tested with t-tests using R[47].

Genetic diversity indexes

We calculated different genetic diversity statistics for each population based on the synonymous SFS as in[21]. Nucleotide diversity (θ_π), Watterson's expected nucleotide diversity (θ_w), and nucleotide diversity in variable sites (π_{var})[22] and Tajima's D[48] were calculated using R. To avoid sampling bias in our results, we divided the variant set into 1,000 equal-sized blocks and performed 1,000 bootstrap iterations of SFSs selecting each time 1,000 random blocks and allowing resampling. This approach bypasses the problem of the stochasticity introduced by independent demographic processes if we were to bootstrap over individuals, as argued in[49].

Variant annotation

The Ensembl Variant Effect Predictor (VEP) version 102[50] was used to annotate the WES variant set, and to assign a functional category to each position. Variants in 5' and 3' UTR regions, downstream, upstream, regulatory, intronic and intergenic regions were considered to have little functional impact and were categorized as synonymous variants. On the other hand, splice site, stop gain and loss variants were considered non-synonymous variants. Additionally, to assess the biological impact of each variant, we also obtained the predicted pathogenicity scores using three different methods: CADD[51], GERP RS[52,53] and Polyphen-2[54] scores. Each of the scores were classified in different categories according to their predicted biological impact. GERP RS scores were stratified in four different classes, −2 to 2, 2 to 4, 4 to 6, and > 6, which have previously[55] been used to assign variants as neutral, weakly, moderately, and strongly deleterious, respectively. CADD scores were stratified into four classes as well: neutral (< 10), weakly deleterious (10 to 20), moderately deleterious (20 to 30), and extreme (> 30). Finally, for Polyphen-2 scores we used three categories: benign (< 0.446), possibly damaging (0.446–0.908), and probably damaging (> 0.908).

Variant frequency distribution

We computed unfolded SFSs using the ancestral-state-annotated WES dataset. VCFtools 0.1.16 was used to count the number of derived and ancestral alleles in each population. The populations were randomly sub-sampled to 20 individuals (the size of the population with fewer samples). Different sets of SFSs were calculated: an SFS using all variants in the dataset and a different SFS per each category within the different annotations (CADD, GERP RS and Polyphen-2).

We summarized the different SFS results by classifying the alleles into low frequency (singletons and doubletons) and common (from tripletons onwards) variants and compared the frequency of each between populations. To avoid sampling bias in our results, we divided the variant set into 1,000 equal sized blocks and performed 1,000 bootstrap iterations of SFSs selecting each time 1,000 random blocks and allowing resampling as proposed by[49].

Mutation load

Differences in mutation load between populations were assessed by calculating two previously used[18–22,25,55] summary statistics for each deleterious category: the number of derived alleles per individual ($N_{alleles}$) and the number of derived homozygotes per individual (N_{hom}). These statistics were calculated per population, and then ratios between populations were calculated. Statistical significance and confidence intervals were calculated, as explained in the section above, by bootstrapping by variant blocks. Quantiles 0.025 and 0.975 of the bootstrapped distributions were used as confidence intervals and the empirical p-value was computed to assess significance. We calculated the mutation load ratios for all the different categories within the three CADD, GERP RS and Polyphen-2 annotations.

DFE inference

The Distribution of Fitness Effect (DFE) was inferred using the ∂a∂i/Fit∂a∂i methods[56,57]. In the absence of a detailed demographic model for our target populations, we tested five different simple demographic models as in[18]: the standard neutral model, a growth model a bottleneck-growth model, a two-epoch model and a three-epoch model. The synonymous SFS was used as an input for the model likelihood estimation since it should putatively represent the neutral variation in the populations. For each population, we selected the model with the highest likelihood (for all populations the best model was the three-epoch model) for the following steps. The inferred demographic parameters (STable 4a) were later used in fit∂a∂i to infer the shape and scale parameters of a gamma DFE per population (STable 4b), which was visualized in different N_e*s discrete bins. The goodness of fit of the selected best likelihood model in ∂a∂i and fit∂a∂i was assessed by comparing the synonymous (∂a∂i) and the non-synonymous (fit∂a∂i) observed and the expected SFSs with χ^2 tests. The confidence intervals for each demographic and DFE parameters were calculated by block bootstrapping the variant set as explained in previous sections.

Demographic parameter estimation

∂a∂i and fit∂a∂i do not estimate the demographic/selection parameters directly, but rather output a set of scaled parameters. For instance, for subsequent analysis we required the scale (E(s)) of the gamma distribution but fit∂a∂i outputs the $E(N_e s)$ parameter. E(s) was calculated as $E(s) = E(N_e s)/N_w$, as in[21] where N_w is the effective population size weighted across time. Considering the best demographic model was the three-epoch model for all populations, N_w was calculated as $N_1 w_1 + N_2 w_2 + N_3 w_3$, were N_i is the effective population size at each epoch i and w_i is a weight assigned for each epoch i, calculated as explained in the supplementary material in[21]. $N_1 = N_{anc}$ was calculated from $\theta_s = 4N_{anc}\mu LS$, where θ_s is the population mutation parameter for synonymous sites estimated by ∂a∂i, $\mu = 1.5 \times 10^{-8}$[58] is the neutral mutation rate, and LS is the number of synonymous sites calculated from L = LNS + LS, where L is the total number of callable sites from where the variants that entered the analysis were called (~ 56 million), and assuming a non-synonymous/synonymous (LNS/LS) ratio of 2.31[57,59]. Since ∂a∂i estimates ratios of effective population size change in each change of epoch (nuB for the second and nuF for the third epoch ratios), N_2 and N_3 were also calculated by multiplying the estimated ratios by N_{anc}, this is: $N_2 = nuB * N_{anc}$ and $N_3 = nuF * N_{anc}$. Similarly, the time estimates were also calculated as $t_2 = TB * 2N_{anc}$ and $t_3 = TF * 2N_{anc}$, being TB the length of the bottleneck and TF the bottleneck recovery time scaled by $2N_{anc}$.

Trajectory of genetic load

To estimate the temporal trajectory of the genetic load we used forward simulations performed with SLiM 3.7.1[60]. As a proxy for a specific demographic model of our populations we used the $IBDN_e$ effective population size curves taking the population size values every 10 generations starting 100 generations ago. Effective population sizes at the last generation (g = 100) were rescaled for IBS and Menorca given the original estimations where unrealistically high. The tree-sequence recording strategy was used to reduce the computational burden produced by neutral mutations as described in the SLiM manual. We simulated genomes consisting of 20 independent chromosomes with 1,000 genes separated by 50,000 bp long neutral non-coding regions. Genes contained eight exon-intron segments, with 100 bp long exons and 5,000 bp long introns. Introns were assumed to be neutral, and exons consisted of 3 bp long codons with the first two positions accepting deleterious mutations and the third being neutral[18,20,21]. The deleterious mutations followed the gamma shaped DFE inferred for each population with fit∂a∂i. The recombination rate was set to 10^{-8} per base per generation and the mutation rate was adjusted from 1.36×10^{-8} to 8.37×10^{-11}, which is the fraction corresponding to nonneutral mutations[18]. We simulated 5,000 generations by setting the population sizes to the inferred N_{anc} as a burn-in phase, and we subsequently calculated the mutation load every five generations as $L = 1 - e^{\sum_i^{anc} l_i}$, where i is each deleterious mutation and $l = s(2hq + q^2(1 - 2h))$, where s is the selection coefficient, q is the frequency of each mutation and h is the dominance coefficient. Two different dominance scenarios were tested: a fully additive model ($h = 0.5$) and a fully recessive model ($h = 0$). Additionally, we also looked at the number of deleterious mutations and number of deleterious homozygotes per individual in each population at the end of the simulations and categorized those mutations according to their selection coefficient in four different classes: from 0 to 10^{-5}, 10^{-5} to 10^{-4}, 10^{-4} to 10^{-3} and $> 10^{-3}$ for slight, moderate low, moderate high, and extreme impact mutations respectively as in[21]. 100 independent simulation replicates were run per population to estimate the confidence intervals of the load trajectories and derived deleterious alleles and homozygotes counts.

Pathogenic variant frequency enrichment

We assessed frequency differences for confirmed and possibly pathogenic variants between Eivissa, Menorca, and IBS. For this purpose, we computed the per-site pairwise F_{ST} for the specific populations using VCFtools 0.1.16. We then identified sites within the top 5% of the F_{ST} values and filtered out synonymous sites (using VEP annotation). Additionally, we selected sites falling within any deleterious category based on GERP, CADD, or Polyphen2 scores described in the Variant annotation section. With this list of differentiated putatively deleterious variants, we searched for clinical evidence of pathogenicity in the ClinVar database[61] by looking at variants with at least one record submitted with an interpretation of "Likely pathogenic" or "Pathogenic" (independent of whether that record includes assertion criteria and evidence).

Results

Genetic structure and ancestral composition

We generated 55 whole-exome sequences for Eivissan and Menorcan individuals, 51 of which passed the quality filters (see Materials and Methods), obtaining a dataset with 874 K exome SNPs. Additionally, 43 samples were also genotyped for the Affymetrix Human Origins array. We assessed the population structure of the modern Eivissans and Menorcans via Principal Component analysis (PCA) and ADMIXTURE (Fig. 1b, c and d) using the WES-Array dataset. Eivissans and Menorcans cluster together with the reference European populations (Fig. 1b) and seem to have little influence from North African or Middle Eastern populations, agreeing with previous results (Biagini et al., 2019) that indicated that Eivissa is a genetic isolate in Europe and discarded a possible genetic continuity in the island from Phoenician times. This might not be the case for some IBS individuals falling between the European cluster and the North African cline. Focusing on the European cluster (Fig. 1c), Eivissa is clearly separated from the Iberian Spanish, and Menorca appears in between them. The ADMIXTURE analysis (Fig. 1d) suggests the differentiation of Eivissa starting in K = 4, where comparing to IBS and Menorca, Eivissa shows a minor presence of a component maximized in Sardinians. In K = 6 an Eivissan ancestral component emerges, which is absent in any other populations except Menorcans, where it makes up for around a third of their total ancestry. These results may reflect patterns of shared isolation and drift in both Balearic Islands, though further evidence is necessary to fully understand the significance of this component.

Interestingly, an individual in IBS seems to have an Eivissanlike ancestry profile, while an Eivissan individual seems to have a Menorcanlike profile.

Expanding on these results, we conducted a series of f-statistics test with Admixtools2 with the aim of exploring shared genetic drift patterns between Eivissa, Menorca and IBS (STable 2). We first explored the *f2* estimates as a measure of dissimilarity between IBS, Menorca and Eivissa. The results show that although Eivissa shows less dissimilarity with Menorca than with IBS, these two seem to be closer to each other than both Balearic populations. We then conducted an *f3* test with our three populations, IBS, Menorca and Eivissa with the aim of testing possible admixture events between Menorca and IBS that could explain the *f2* results. The *f3* results for all population combinations yielded positive values, suggesting limited or no admixture between them. These results again indicate that the dissimilarity between Eivissa and Menorca is higher than between the former and IBS. This is a result that could also be concordant with a significant genetic drift occurring in the Eivissan branch after the split with Menorca, and not just with Menorca and IBS lying on the same branch after the separation of Eivissa. Next, we conducted an outgroup *f3* test using the Mozabite (we also obtained comparable results with Mbuti, data not shown) as an outgroup and rotating between IBS, Eivissa and Menorca in order to see the shared drift/genetic similarity between these populations. The results show the highest shared drift between Menorca and Eivissa, indicating that the Balearic populations may form a clade. This is finally confirmed in the *f4* testing for the 'treeness' of the following configuration: Mozabite splitting first, IBS second, and finally the Eivissa-Menorca split. The result is not significatively different from 0, indicating that Eivissa and Menorca form a clade with respect to IBS and Mozabite (regardless of how the former two populations branch between themselves).

In this regard, we checked for a possible differential ancestral composition in Eivissans compared to IBS and Menorcans, by modelling modern populations using ancient samples. We performed a distal five-way admixture model with qpAdm with the following source populations: Western Hunter Gatherers (WHG), Steppe pastoralists (Yamnaya_Samara), Anatolian Neolithic (Anatolia_N), Iranian Neolithic (Iran_N) and Late Neolithic Moroccoans (Morocco_LN) (see STable 3 for details) emulating previous studies (Fernandes et al., 2020), with the aim of representing the main ancestral sources that constituted the genetic diversity in the Western Mediterranean. The results evidence the differential Anatolian Neolithic component present in modern Sardinians and the minor presence of North African or Iranian-related ancestry in CEU (also fitting models without Morocco_LN and Iran_N), but detect no significant differences between present day Balearic and Iberian populations (STable 3). This result suggests a recent differentiation between present day Iberian and Balearic populations and does not fit with a possible differential Central European influence in modern Eivissans that could be suggested in the K = 4 ADMIXTURE result.

Demographic parameters and genetic diversity

Since genetic isolation and drift were suggested to be the reason of the differentiation of Eivissa[14], we estimated the change of effective population size (N_e) along time with $IBDN_e$ using the WES-Array variant set. The results show that both Eivissa and Menorca experienced a recent progressive reduction of the Ne approximately between 50 and 20 generations ago, that is more extreme in Eivissa (SFigure 3 and SFigure 4a-b), followed by a recent extreme increase detected in all analyzed populations. Sardinians, another genetic isolate in the Mediterranean, have maintained a reduced but constant recent population size, and, on the contrary, IBS presents a subtle increase over recent history. In addition, we ran the ASCEND software on the WES-Array data with Eivissa and Menorca as target populations. The results detect a founder effect occurring ~ 20 generations ago (~ year 1500 CE), with a stronger intensity in Eivissa (~ 0.8%) than in Menorca (~ 0.3%) (SFigure 4a-b). Overall, these figures are consistent with the results obtained with $IBDN_e$ regarding both the timing and the relative intensities in the founder effects of both Islands.

In agreement with these results, the different diversity indexes calculated (SFigure 5a-d) also evidence slightly lower genetic diversity levels (mainly reflected in the Watterson's theta estimator (θ_w), Tajimas's D and nucleotide diversity of variable sites (π_{var})) in Eivissa compared to Menorca and IBS and around the values of Sardinia. North African and Middle Eastern populations show overall higher diversity, probably due to the gene flow from sub-Saharan populations.

ROHs and IBD fragment analyses

We further looked into the degree of isolation and inbreeding by analyzing the runs of homozygosity (ROHs) and identity-by-descent (IBD) fragments using the WES-Array variant set. The overall number of ROHs (SFigure 6a) and the total sum of the ROH length (SFigure 6b) per individual shows Eivissa contains more ROHs and consequently, a larger fraction of their genomes is constituted by ROH segments when comparing to IBS. The figures are comparable to those of other genetic isolates such as Sardinians or Mozabite. In these results, Menorca seems to have a slightly higher number of ROHs than IBS but the difference is not significant ($P = 0.62$). We also divided the ROHs in three different length categories (1-2.5 Mb, 2.5-5 Mb and > 5 Mb) (Fig. 2), and observed differences between Eivissa and IBS/Menorca in the short (1-2.5 Mb), and mainly, in the intermediate length (2.5-5 Mb) categories. Some Eivissan individuals carry a few long ROHs, but this is a pattern observed also in general IBS individuals (SFigure 7). This suggests that recent, close consanguinity might not be playing a differential role in Eivissans compared to IBS, and that the overall pattern of ROHs is more consistent with inbreeding and a historically reduced effective population size.

Regarding IBD segments, Eivissa shows the second highest mean number of intrapopulation IBDs after the Mozabite, suggesting higher levels of inbreeding (SFigure 8). Menorca also shows higher values of intrapopulation IBDs than general European populations. The average length of the IBD segments in Eivissa is similar to the values in the rest of populations except for Palestinians, where the sum of shared IBDs is highly heterogeneous, with some individuals probably sharing very long IBDs (SFigure 9).

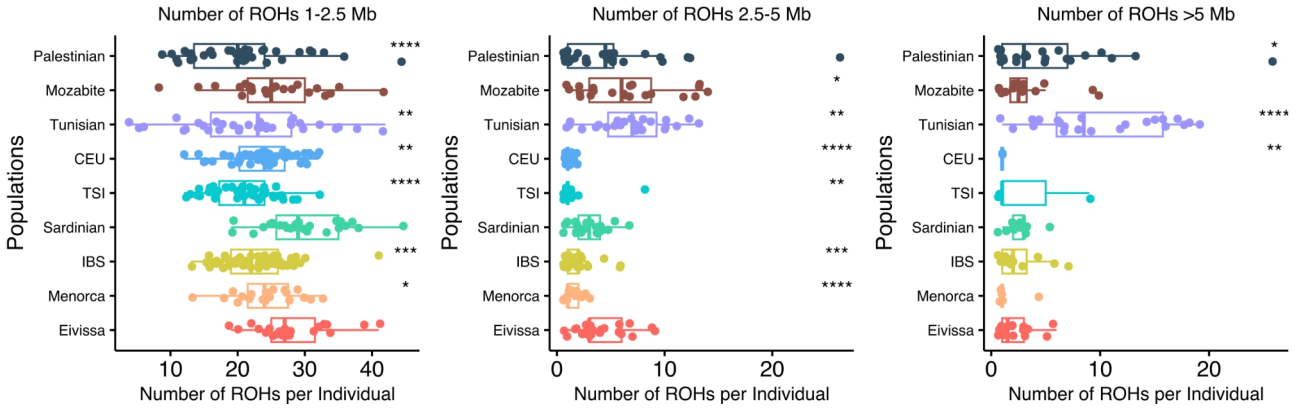

Fig. 2. Number of runs of homozygosity (ROHs) per individual divided by size categories. Statistical significance was assessed with t-tests using Eivissa as the fixed group: * $P<0.05$, ** $P<0.01$, *** $P<0.001$, **** $P<0.0001$.

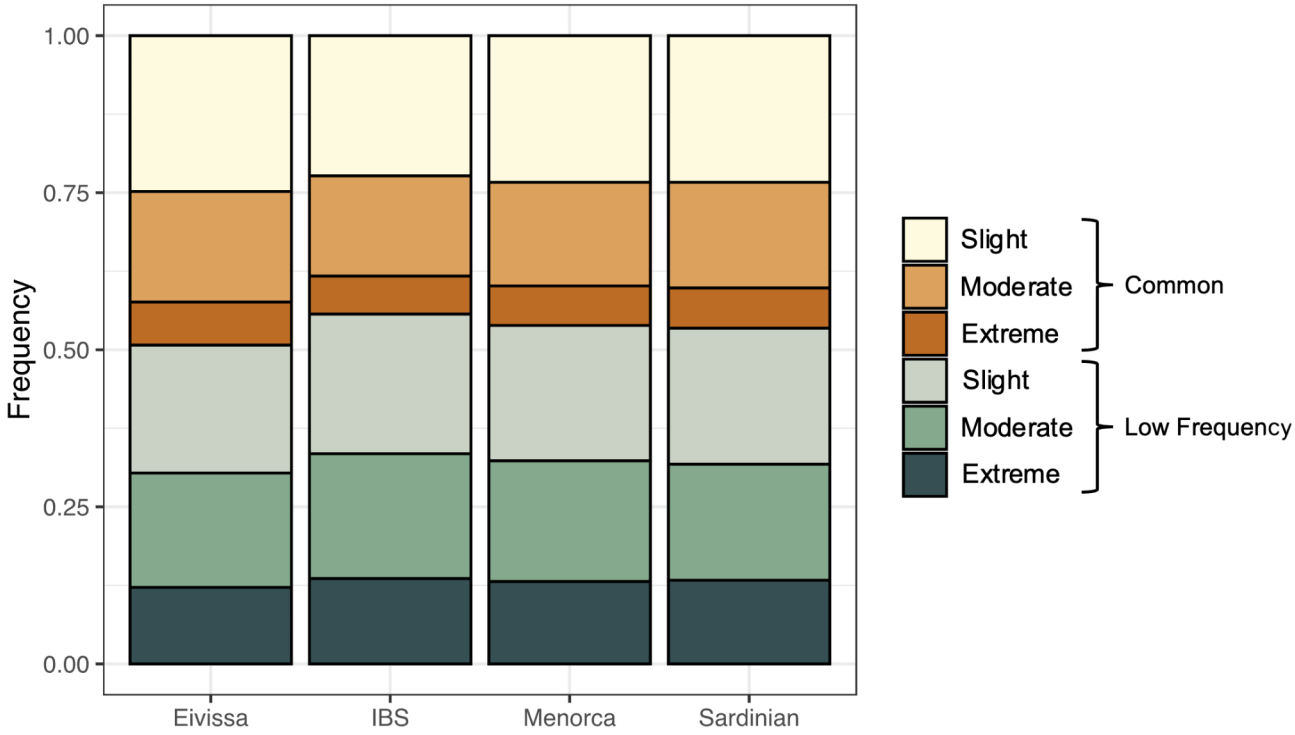

Fig. 3. Proportion of low-frequency (singletons and doubletons) and common (tripletons and onwards) derived alleles for the three deleterious categories based on GERP scores. Slightly deleterious for $2<\text{GERP}\leq 4$, moderately deleterious for $4<\text{GERP}\leq 6$ and extremely deleterious for $6<\text{GERP}$.

Frequency distribution of functional variants

It is known that different evolutionary processes such as genetic drift or selection can significantly influence variant allele frequencies. For this reason, we assessed the frequency distribution of our exomic variant set using the site frequency spectra (SFS), and we analyzed them by dividing the variants according to their functional impact (SFigs. 10, 11 and 12). The SFS results show that, for all deleterious categories, Eivissa presents a flatter SFS when comparing to IBS, Menorca or Sardinia, mainly due to a slight depletion of singletons that is compensated in larger frequency bins such as doubletons and tripletons. This can also be observed when pooling all common (tripletons and larger frequency variants) and low-frequency (singletons and doubletons) variants, and when using all GERP, CADD and Polyphen2 annotations (Fig. 3, SFigs. 13, 14 and 15, STable 5). Overall, rare variants are less frequent in Eivissa, regardless of deleteriousness category, even when compared to Sardinians. This pattern extends also to the presumably neutral variants (SFigure 15). Furthermore, as the deleteriousness of the variant categories increases, we detect a decrease in the differences in proportion of both common and

rare variants between Eivissa and the rest of the populations (STable 6), suggesting that selection acts reducing those differences as the deleteriousness of variants increases. Altogether, the differences observed might be the consequence of the lower effective population sizes in recent times and the subsequent genetic drift increasing the proportion of rare variants for both neutral and deleterious categories. This is compatible with the reduction of the effective population size in Eivissa not leading to a loss of the efficacy of purifying selection, at least for values of the selection coefficient large enough to be predicted by the deleteriousness estimation algorithms.

Mutation load

As explained above, Eivissans have slight differences in the frequency distribution of deleterious and neutral variants. In relation to this, recent demography has been shown to affect not only the frequency distribution of variants but also the amount of deleterious variants carried by populations (i.e., the mutation load)[18–20]. To gain further insight into the deleterious burden in Eivissa, we estimated the mutation load, with previously used estimators, for each deleterious category (using all GERP, CADD and Polyphen2 annotations), and under two different dominance models: assuming all variants are additive (calculating the number of derived alleles, $N_{alleles}$), and assuming all variants are recessive (calculating the number of derived homozygotes, N_{hom}) (Fig. 4, SFigs. 16 and 17). The block bootstrap replicates show there are no important differences in the amount of deleterious alleles or deleterious homozygotes carried by the studied populations for any of the deleterious categories, although some of the means of these replicates statistically differ from 1 (STable 7). These suggests the excess of common deleterious variants might be compensated by the lack of rare deleterious variants in Eivissa, resulting in a comparable overall number of deleterious variants when compared to the rest of populations.

Following these results, we measured the ratio of deleterious to synonymous homozygotes in and outside ROHs, since previous studies have found that ROHs are enriched in deleterious homozygous variants[62]. For most populations, including Eivissa, we found no significant enrichment in deleterious homozygotes inside ROHs comparing to outside ROHs probably due to the reduced number of samples analyzed (SFigures 18–19).

These estimations of mutation load are limited, among other factors, by the accuracy of the deleteriousness predictions and by the lack of information of the dominance coefficient of every deleterious variant[23]. In this context, simulations are a powerful tool to test different dominance and demographic scenarios. With this in mind, we used SLiM to perform forward simulations to study the change of the mutation load across time and under fully additive and fully recessive dominance scenarios. In order to achieve this, we required an estimation of the distribution of fitness effects (DFE) of new deleterious mutations, for which we used ∂a∂i[56] to infer three-epoch demographic models (STable 4a, SFigure 20), which were then used to infer the parameters of gamma shaped DFE for each of the analyzed populations (STable 4b, SFigure 21). The resulting DFEs are very similar between populations, with most of the new mutations falling in the neutral or strongly deleterious ranges

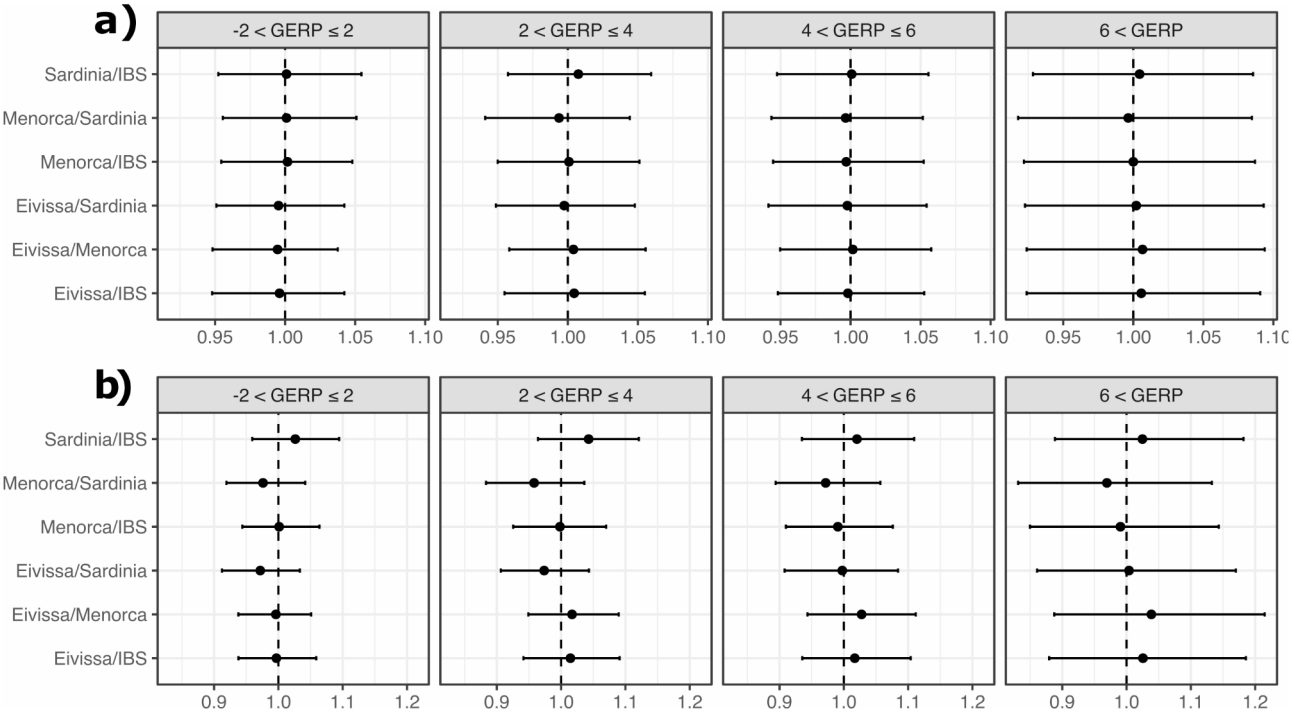

Fig. 4. (**a**) Population ratios of the total number of deleterious derived alleles. (**b**) Population ratios of the total number of deleterious derived homozygotes. Results are divided in the four deleterious categories: neutral for $-2 \leq GERP \leq 2$, slightly deleterious for $2 < GERP \leq 4$, moderately deleterious for $4 < GERP \leq 6$ and extremely deleterious for $6 < GERP$. Error bars were built with the 0.025 and 0.975 quantiles of the block bootstrap replicates.

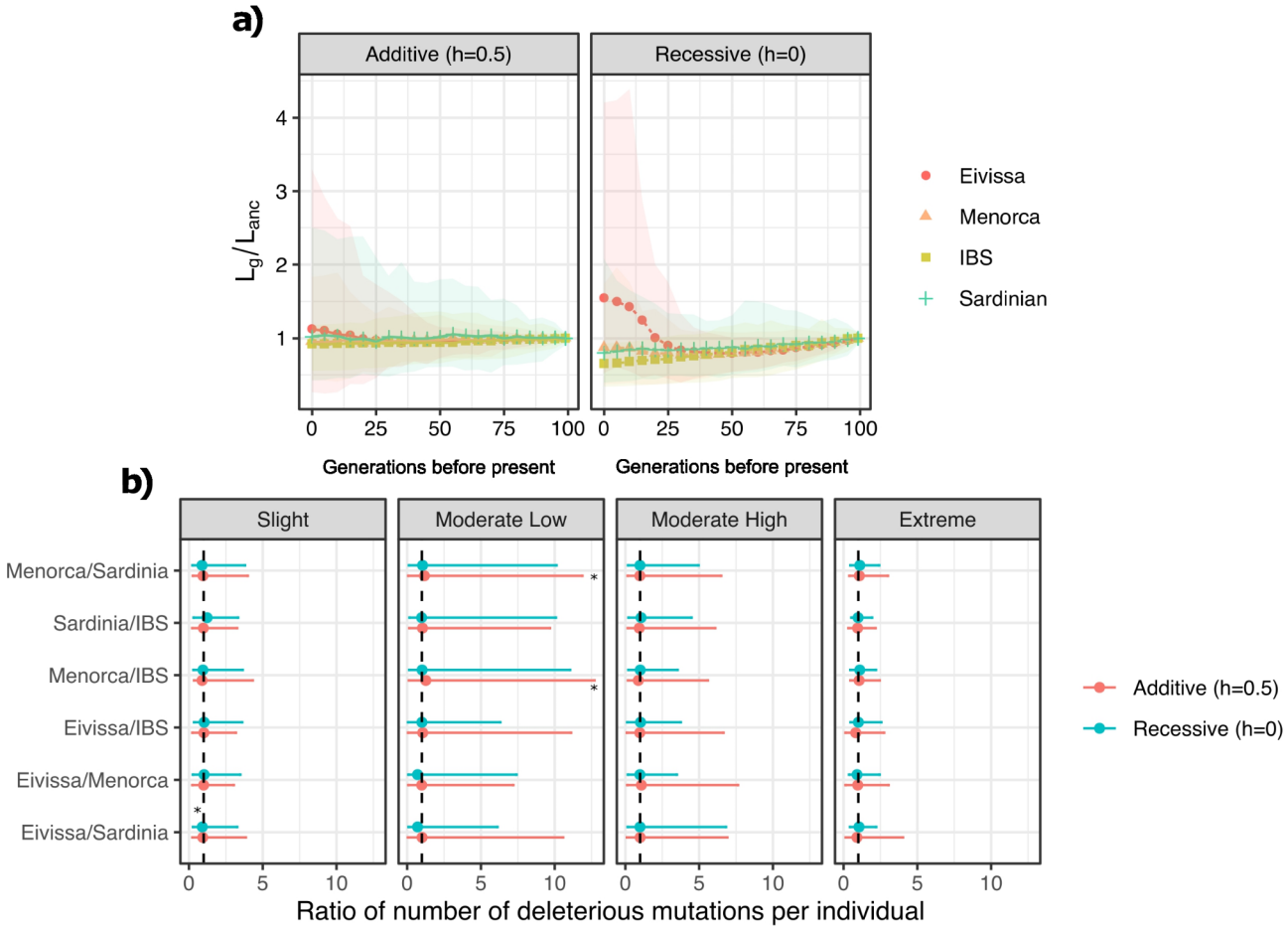

Fig. 5. (**a**) Time trajectory of the relative mutation load obtained by dividing the load in each generation (Lg) by the ancestral load (Lanc). The shadowed area represents the 2.5% and 97.5% quantiles of the distribution generated in 100 simulations. (**b**) Trajectory of the width of the lower and upper quantiles from figure a). (**c**) Simulated ratios between pairs of populations of the number of deleterious mutations per individual. Error bars were built with the 2.5% and 97.5% quantiles of the 100 simulation replicates. Deleterious categories were divided in: slight ($0 < s \leq 10e\text{-}5$), moderate low ($10e\text{-}5 < s \leq 10e\text{-}4$), moderate high ($10e\text{-}4 < s \leq 10e\text{-}3$) and extreme ($10e\text{-}3 < s \leq 1$). Statistical significance is shown the following way: * ($P > 0.01$).

(SFigure 22). These DFE were then used, together with the effective population size trajectories inferred with IBDNe, to run the forward simulations.

In order to inspect possible load changes in time, we calculated the relative mutation load dividing the mutation load every five generations by the ancestral load (Fig. 5a). Under an additive model, the mutational load stays relatively constant across time for all populations, whereas under a recessive model, the mutation load slightly decreases with time for all populations except for Eivissa, where around 30 generations before present, the relative load starts to increase reaching a median of 1.6 times higher load relative to the ancestral (Fig. 5a). It should be noted that despite the large range covered by the 2.5% and 97.5% quantiles for the relative load estimates indicating the differences in relative loads between populations might not be substantial, differences in both the absolute and relative load between Eivissa and the other populations in the last generation of the simulations are significant under the recessive model (SFigure 23a-b). Furthermore, the width of these confidence intervals increases considerably in populations that have suffered stronger bottlenecks (SFigure 24), evidencing the importance of chance selecting deleterious variants in population bottlenecks.

In order to better compare these results with our observed mutation load estimates, we also calculated the population ratios of the number of deleterious mutations per individual at the final generation of the simulations (Fig. 5b). We observe that most of the median values of the simulated ratios are ~ 1 for all categories in both the additive and the recessive models with a few exceptions being significantly different (Fig. 5b, STable 8), which suggests no considerable differences in mutation load between the populations analyzed. This overall lack of difference in load observed when counting the number of deleterious alleles appears to contrast with the slight load increase observed in the load trajectory under the recessive model for Eivissa, and thus, indicates that different results can arise when using two different load statistics (the number of derived alleles or mutations, N_{allele} and the load formula, $L = 1 - e^{\sum_i l_i}$).

Putting the simulation results in context with the observed load ratios, we have observed that, on the one hand, Eivissans seem to present a slight relative load increase under a recessive model, while on the other hand, differences in the amount of deleterious mutations observed between the populations analyzed are not statistically significant, neither in the simulated data nor in the observed data. This discordance might be partly explained by the use of different statistics to measure load. With this in mind, despite not observing a significant difference in the total number of deleterious alleles in Eivissans nor Menorcans when compared to the reference populations, our results show that genetic drift has caused deleterious variants to have higher frequencies in Eivissa, and to a lesser extent in Menorca, when comparing with IBS, which could result in an enrichment of certain pathogenic variants.

Pathogenic variant frequency enrichment

Further to the latter point, we analyzed frequency differences of possibly deleterious variants and looked into their implications for health and disease, for which we checked the clinical evidence of each possibly pathogenic variant in the ClinVar database[61]. When comparing Eivissa and IBS we find three missense variants with clinical evidence for health consequences in genes *ACKR1*, which causes the Fy(bwk) phenotype in the Duffy group system and provides protection against the infection by *Plasmodium vivax*, *DNAI1* associated with a ciliary dyskinesia, and SLC29A3 which alters the response in gemcitabine-based chemotherapy (STable 9). When comparing Menorca and IBS we find three other missense variants in genes *PDE6A*, *NECTIN3* and *USH2A* involved in eye diseases (STable 9). All of these variants except for those on genes *SLC29A3* and *ACKR1* are located in IBD segments shared by the Eivissan and Menorcan carriers.

Discussion

Recent studies showed that modern Eivissans present signs of genetic isolation that are absent in other Balearic populations[14]. With this in mind, we generated new exome sequence data from 31 individuals from Eivissa and 20 individuals from Menorca, with the aim of assessing the effects of presumably different recent demographic histories in the functional variation.

Our results show Eivissans differentiate clearly from the Spanish general population, agreeing with the latest study[14]. However, and unnoticed so far, we also observe the Menorcan individuals separate from the Iberian Spanish cluster, as they fall towards Eivissans in the PCA indicating shared drift between both Balearic populations. Despite some studies suggested a genetic continuity between Phoenicians and modern Eivissans[12,13], our results do not show differential Middle Eastern or North African influence compared to other south-western Mediterranean populations. This agrees with the results from the latest genome-wide studies[14], indicating the genetic origin of present-day Eivissan and Menorcan individuals could possibly be mostly attributed to the settlement that followed the conquest of the Balearic Islands in the 13th century by the crown of Aragon. On this regard, although precise records about the origin of these settlers are missing for Eivissa and Menorca, the number of individuals coming from rural areas of Catalonia registered in Mallorca[9] suggests the absolute contribution of Catalan settlers could have also been relevant in Eivissa and Menorca, when considering their reduced population sizes (around 2,300 and 3,600 respectively, in the first tax census in the year 1329[63]). We also detect some degree of shared genetic drift between Menorca and Eivissa as shown in Fig. 1c and d or in the IBD sharing analyses (SFigs. 7 and 8). This shared drift could have originated in the founder Catalan population (perhaps also in the repopulation of Mallorca, whose influence was surely important in the demography of the Balearic Islands[8]), having been then preserved and exacerbated in the smaller and more isolated island of Eivissa and partially diluted by subsequent gene flow with external populations in Menorca. Another possibility, although less likely, is that the pre-conquer islanders, with so far an understudied genetic background, had maintained a pre-Phoenician Western Mediterranean component relatively uninfluenced by historic Middle Eastern or North African gene flow, whereby creating a more ancient shared genetic drift. However, the recent reduction of genetic diversity evidenced by the inferred IBDNe trajectory (SFigure 3) suggests drift occurred recently rather than in pre-Phoenician times, which aligns more closely with the first hypothesis. The timing of this recent effective population size reduction is consistent with a founder effect in the repopulation of the islands after the invasion by the Aragonese crown, although other recent historical events such as the Franco-Ottoman attacks in the 16th century[64] or the bubonic plague epidemics in the 17th century could have also contributed to the reduction of the effective population size. Since the number of ancient DNA samples from the Balearic Islands is reduced, future studies in this field will help to ascertain the genetic composition of Balearic inhabitants during different periods and assess the genetic effects of demographic changes over time.

We next explored the functional consequences of the demographic history in Eivissa and Menorca. Eivissa shows a higher number of short and intermediate size ROHs when compared to IBS, typically associated to a background of parental relatedness due to a limited population size (Gibson 2006), while for Menorca, just a slight difference with IBS is observed in the number of short ROHs. This is consistent with the $IBDN_e$ inferences and the calculated genetic diversity statistics, indicating a genetic diversity reduction due to a limited population size, which in the case of Eivissa is consistent with the reported increase of isonymy (reduction of name and surname diversity)[65] and frequency of consanguineous unions[10], something that occurred probably to a lesser extent in Menorca as a result of experiencing less isolation.

When analyzing the frequency of deleterious variants, the Mediterranean islands analyzed present a flattening of the SFS (i.e. decrease in the proportion of rare variants), when compared to IBS (Fig. 3), being Eivissa the population with the flattest SFS. This suggests a further reduction of population size in Eivissa, which according to the $IBDN_e$ through time results, presumably occurred during medieval times. This flattening of the SFS has also been observed in other bottlenecked genetic isolates[18–22]. In addition, the fact that the differences of common and rare variant proportions between populations decreases as the predicted deleteriousness of variants

increases, indicates the efficiency of purifying selection has not been totally compromised after population size reductions. This pattern has also been observed in genetic isolates such as European Roma[20].

Given its demographic history, we next tested for a possible differential accumulation of deleteriousness (i.e. mutation load) in Eivissa compared to the rest of populations analyzed. Since the information about precise selection coefficient values of each allele (i.e. deleteriousness) and dominance coefficient are not known, the empirical calculation of the mutation load is impossible with genomic data[23]. We, therefore, calculated two different previously used statistics[18–22,55] thought to reflect the mutation load under two different dominance assumptions: the number of derived deleterious alleles per individual ($N_{alleles}$), which reflects the load under a fully additive dominance model, and the number of derived deleterious homozygotes per individual (N_{hom}) reflecting the load under a fully recessive model of dominance. Our results show that the number of deleterious derived alleles or of homozygotes are not different between Eivissa and the rest of the populations, thus suggesting the genetic load is similar between the studied populations under both fully additive and recessive dominance models, which in turn reflects that the efficiency of purifying selection has been kept despite effective population size changes. Therefore, the frequency increase in common deleterious variants in Eivissa seems to be balanced by the lack of rare variation, resulting in a similar absolute number of deleterious alleles and homozygotes.

These results are dependent on the accuracy of the functional annotation capturing the actual selection coefficient of each derived allele. To overcome this challenge, we performed forward simulations under both fully additive and recessive models, after inferring a gamma shaped DFE to determine the distribution of selection coefficients of the simulated variation. In the absence of a complete demographic model for the analyzed populations, a set of 100 simulation replicates were performed using the inferred $IBDN_e$ trajectories. For each population, we calculated the genetic load trajectory relative to the ancestral load of each population (see Materials and Methods). The results evidence the small influence demographic history has had on load under a fully additive model, while for the fully recessive model, the mean value of the replicates for Eivissa indicates the demographic history of this population has resulted in an accumulation of deleterious variants relative to its ancestral state. It should be noted that the variation between the replicates increases in each population with the strength of their effective population size reduction. This evidences that although, on average, population bottlenecks result in an increased load, chance plays a main role selecting more or less damaging variants. This variation between replicates is again observed when looking at the simulated $N_{alleles}$ per population, where differences between populations are generally not significant, regardless of the dominance model.

Overall, when putting in context the relative load with both the simulated $N_{alleles}$ and the observed $N_{alleles}$ and N_{hom} ratio statistics, opposing load interpretations arise. While Eivissa seems to present an increase in the recessive load, this is not reflected in the amount of deleterious mutations ($N_{alleles}$) carried by each population, neither in the simulated data nor in the observed data. This indicates the choice of load statistic might be important when trying to infer population differences in mutation load, being some statistics more sensitive than others. Estimating the mutation load is challenging and carries some limitations. The load estimated from the observed data is dependent on the accuracy of deleteriousness predictions, while model-based simulations might be affected by an oversimplification of the demographic models used. For this reason, we favor the use of different statistics and approaches to try to understand the impact of demography in the mutation load of populations. Altogether, our results suggest that if there is any increase in the recessive load in Eivissa compared to other populations, this load is difficult to detect in the observed data.

Regardless of whether the mutation load is higher in Eivissa, our findings indicate that population history has significantly influenced the way this load is manifested, since, as seen previously, Eivissans have fewer polymorphic sites, but derived allele frequencies at those polymorphic sites are usually slightly higher. This also applies to deleterious variation, having therefore, potential relevant medical implications. Despite the lack of reports of higher incidences of diseases in Eivissa or of founder mutations, we looked for the most frequency differentiated deleterious variants between Eivissa, Menorca and IBS in the medical literature, and found different missense variants reported to be clinically relevant.

Finally, after Eivissa was discovered to be a genetic isolate in the Mediterranean, we wanted to further expand on its demographic history and assess its functional consequences comparing the results with Menorca, given their similar sizes and proximity. We show both islands, with Eivissa showing stronger signals, differentiate from the Spanish general population given to the genetic drift undergone in recent history. This demographic history has also affected the functional genetic variation increasing the frequencies of common variants. These frequency shifts, however, appear not to have considerably changed the total deleterious burden of Eivissa when compared to other populations. These results, although limited by a reduced sample size, evidence the importance of considering different population histories in biomedical studies and could serve as a starting point for future research further characterizing the medical genetic landscape of understudied populations.

Data availability

Eivissan and Menorcan exome sequences and Affymetrix Human Origins genotypes have been deposited et EGA with accession numbers: EGAD50000000620 and EGAD50000000614 respectively.

Received: 2 July 2024; Accepted: 23 December 2024
Published online: 03 January 2025

References

1. Cherry, J. F. & Leppard, T. P. The Balearic Paradox: why were the islands colonized so late? *Pyrenae* **49**, 49–70 (2018).
2. Fernandes, D. M. et al. The spread of steppe and iranian-related ancestry in the islands of the western Mediterranean. *Nat. Ecol. Evol. 2020.* **4**(3), 334–345 (2020).

3. Sureda, P. et al. El Poblado Naviforme De cap de Barbaria II (Formentera, Islas Baleares). Nuevos datos sobre su cronología y secuencia de ocupación. *Trabajos De Prehistoria*. **74**, 319–334 (2017).
4. Guerrero Ayuso, V. M., Calvo Trias, M. A., García Rosselló, J. & Gornés Hachero, J. S. Prehistoria de las Islas Baleares: registro arqueológico y evolución social antes de la Edad de Hierro. *Prehistoria de las Islas Baleares = Prehistory of the Balearic Islands: Registro Arqueológico y Evolución Social antes de la Edad del Hierro = Archaeological Record and Social Evolution Before the Iron Age* 185–250 (2007).
5. Aubet, M. & Eugenia *The Phoenicians and the West: Politics, Colonies and Trade* (Cambridge University Press, 2001).
6. Benjamí Costa Ribas & & Jordi, H. Fernández Gómez. Eivissa-història-època feniciopúnica. *Enciclopèdia d'Eivissa i Formentera* (2024).
7. Gurrea Barricarte, R. & Martín Parrilla, Á. Eivissa-Història-Època Andalusina. *Enciclopèdia d'Eivissa i Formentera* (2024).
8. Serra Belabre, M. L., Rosselló Bordoy, G. & Orfila León, J. A. & de Nicolás Mascaró, J. C. Historia de Menorca (1977).
9. Mas Forners, A. El procés repoblador a Mallorca durant la primera meitat del segle XIV. Una aportació al seu estudi. *Bolletí de la Societat Arqueològica Lul·liana: Revista d'Estudis Històrics, ISSN 0212–7458, No. 50*, 167–198 (1994).
10. von Alarco, C. Sobre los matrimonios consanguíneos en Ibiza. *Eivissa, ISSN 1130–7803, ISSN-e 2385–3476, No. 8*, 16–19 (1976).
11. Bisson, J. La propiedad ciudadana en las Islas Baleares. *Treballs de geografia, ISSN 1133-181X, No.* 9 1–14 (1972).
12. Picornell, A., Gómez-Barbeito, L., Tomàs, C., Castro, J. A. & Ramon, M. M. Mitochondrial DNA HVRI variation in Balearic populations. *Am. J. Phys. Anthropol.* **128**, 119–130 (2005).
13. Tomàs, C., Jiménez, G., Picornell, A., Castro, J. A. & Ramon, M. M. Differential maternal and paternal contributions to the genetic pool of Ibiza Island, Balearic Archipelago. *Am. J. Phys. Anthropol.* **129**, 268–278 (2006).
14. Biagini, S. A. et al. People from Ibiza: an unexpected isolate in the Western Mediterranean. *Eur. J. Hum. Genet.* **27**(6), 941–951 (2019).
15. Zalloua, P. et al. Ancient DNA of Phoenician remains indicates discontinuity in the settlement history of Ibiza. *Sci. Rep.* **8**(1), 1–15 (2018).
16. Somers, M. et al. A genetic population isolate in the Netherlands showing extensive haplotype sharing and long regions of homozygosity. *Genes*. **8**, 133 (2017).
17. Casals, F. et al. Whole-exome sequencing reveals a rapid change in the frequency of rare functional variants in a founding population of humans. *PLoS Genet.* **9**, e1003815 (2013).
18. Lucas-Sánchez, M. et al. The impact of recent demography on functional genetic variation in north African human groups. *Mol. Biol. Evol.* **41**, (2024).
19. Lucas-Sánchez, M., Font-Porterias, N., Calafell, F., Fadhlaoui-Zid, K. & Comas, D. Whole-exome analysis in Tunisian Imazighen and Arabs shows the impact of demography in functional variation. *Sci. Rep.* **11**(1), 1–16 (2021).
20. Font-Porterias, N. et al. The counteracting effects of demography on functional genomic variation: the Roma paradigm. *Mol. Biol. Evol.* **38**, 2804 (2021).
21. Lopez, M. et al. The demographic history and mutational load of African hunter-gatherers and farmers. *Nat. Ecol. Evol. 2018.* **2**(4), 721–730 (2018).
22. Pedersen, C. E. T. et al. The effect of an extreme and prolonged population bottleneck on patterns of deleterious variation: insights from the Greenlandic Inuit. *Genetics* **205**, 787–801 (2017).
23. Henn, B. M., Botigué, L. R., Bustamante, C. D., Clark, A. G. & Gravel, S. Estimating the mutation load in human genomes. *Nat. Rev. Genet.* **16**, 333–343 (2015).
24. Do, R. et al. No evidence that selection has been less effective at removing deleterious mutations in Europeans than in Africans. *Nat. Genet.* **47**(2), 47–126 (2015).
25. Simons, Y. B., Turchin, M. C., Pritchard, J. K. & Sella, G. The deleterious mutation load is insensitive to recent population history. *Nat. Genet.* **46**(3), 220–224 (2014).
26. Chiang, C. W. K. et al. Genomic history of the Sardinian population. *Nat. Genet.* **50**(10), 1426–1434 (2018).
27. Bolger, A. M., Lohse, M. & Usadel, B. Trimmomatic: a flexible trimmer for Illumina sequence data. *Bioinformatics* **30**, 2114–2120 (2014).
28. Andrews, S. FastQC A Quality Control tool for high throughput sequence data. *Babraham Bioinf.* https://www.bioinformatics.babraham.ac.uk/projects/fastqc/ (2010).
29. Van der Auwera, G. A. et al. From FastQ data to high-confidence variant calls: the genome analysis toolkit best practices pipeline. *Curr. Protoc. Bioinf.* **43**, 11101–111033 (2013).
30. Li, H. & Durbin, R. Fast and accurate short read alignment with Burrows–Wheeler transform. *Bioinformatics* **25**, 1754–1760 (2009).
31. Li, H. et al. The sequence Alignment/Map format and SAMtools. *Bioinformatics* **25**, 2078–2079 (2009).
32. Broad Institute. Picard toolkit. Broad Institute, GitHub repository (2018).
33. Okonechnikov, K., Conesa, A. & García-Alcalde, F. Qualimap 2: advanced multi-sample quality control for high-throughput sequencing data. *Bioinformatics* **32**, 292–294 (2016).
34. Auton, A. et al. A global reference for human genetic variation. *Nature* **526**(7571), 68–74 (2015).
35. Danecek, P. et al. The variant call format and VCFtools. *Bioinformatics* **27**, 2156–2158 (2011).
36. Manichaikul, A. et al. Robust relationship inference in genome-wide association studies. *Bioinformatics* **26**, 2867 (2010).
37. Purcell, S. et al. PLINK: a tool set for whole-genome association and population-based linkage analyses. *Am. J. Hum. Genet.* **81**, 559 (2007).
38. Patterson, N., Price, A. L. & Reich, D. Population structure and Eigenanalysis. *PLoS Genet.* **2**, e190 (2006).
39. Alexander, D. H., Novembre, J. & Lange, K. Fast model-based estimation of ancestry in unrelated individuals. *Genome Res.* **19**, 1655 (2009).
40. Behr, A. A., Liu, K. Z., Liu-Fang, G., Nakka, P. & Ramachandran, S. Pong: fast analysis and visualization of latent clusters in population genetic data. *Bioinformatics* **32**, 2817–2823 (2016).
41. Mallick, S. & Reich, D. The Allen Ancient DNA resource (AADR): a curated compendium of ancient human genomes. https://doi.org/10.7910/DVN/FFIDCW (2023).
42. Patterson, N. et al. Ancient admixture in human history. *Genetics* **192**, 1065–1093 (2012).
43. Browning, B. L., Tian, X., Zhou, Y. & Browning, S. R. Fast two-stage phasing of large-scale sequence data. *Am. J. Hum. Genet.* **108**, 1880–1890 (2021).
44. Browning, B. L. & Browning, S. R. Improving the accuracy and efficiency of identity-by-descent detection in population data. *Genetics* **194**, 459–471 (2013).
45. Browning, S. R. & Browning, B. L. Accurate non-parametric estimation of recent effective population size from segments of identity by descent. *Am. J. Hum. Genet.* **97**, 404–418 (2015).
46. Tournebize, R., Chu, G. & Moorjani, P. Reconstructing the history of founder events using genome-wide patterns of allele sharing across individuals. *PLoS Genet.* **18**, e1010243 (2022).
47. R Core Team. *R: A Language and Environment for Statistical Computing*. https://www.R-project.org/ (2021).
48. Kousathanas, A., Oliver, F., Halligan, D. L. & Keightley, P. D. Positive and negative selection on noncoding DNA close to protein-coding genes in wild house mice. *Mol. Biol. Evol.* **28**, 1183–1191 (2011).
49. Simons, Y. B. & Sella, G. The impact of recent population history on the deleterious mutation load in humans and close evolutionary relatives. *Curr. Opin. Genet. Dev.* **41**, 150–158 (2016).

50. McLaren, W. et al. The Ensembl variant effect predictor. *Genome Biol.* **17**, 1–14 (2016).
51. Rentzsch, P., Witten, D., Cooper, G. M., Shendure, J. & Kircher, M. CADD: predicting the deleteriousness of variants throughout the human genome. *Nucleic Acids Res.* **47**, D886–D894 (2019).
52. Cooper, G. M. et al. Distribution and intensity of constraint in mammalian genomic sequence. *Genome Res.* **15**, 901 (2005).
53. Davydov, E. V. et al. Identifying a high fraction of the human genome to be under selective constraint using GERP++. *PLoS Comput. Biol.* **6**, 1001025 (2010).
54. Adzhubei, I. A. et al. A method and server for predicting damaging missense mutations. *Nat. Methods.* **7**, 248 (2010).
55. Henn, B. M. et al. Distance from Sub-saharan Africa predicts mutational load in diverse human genomes. *Proc. Natl. Acad. Sci. USA.* **113**, E440–E449 (2016).
56. Gutenkunst, R. N., Hernandez, R. D., Williamson, S. H. & Bustamante, C. D. Inferring the joint demographic history of multiple populations from multidimensional SNP frequency data. *PLoS Genet.* **5**, e1000695 (2009).
57. Kim, B. Y., Huber, C. D. & Lohmueller, K. E. Inference of the distribution of selection coefficients for new nonsynonymous mutations using large samples. *Genetics* **206**, 345–361 (2017).
58. Ségurel, L., Wyman, M. J. & Przeworski, M. Determinants of mutation rate variation in the human germline. *Annu. Rev. Genomics Hum. Genet.* **15**, 47–70 (2014).
59. Huber, C. D., Kim, B. Y., Marsden, C. D. & Lohmueller, K. E. Determining the factors driving selective effects of new nonsynonymous mutations. *Proc. Natl. Acad. Sci. U S A.* **114**, 4465–4470 (2017).
60. Haller, B. C. & Messer, P. W. SLiM 3: forward genetic simulations beyond the Wright–Fisher model. *Mol. Biol. Evol.* **36**, 632–637 (2019).
61. Landrum, M. J. et al. ClinVar: public archive of relationships among sequence variation and human phenotype. *Nucleic Acids Res.* **42**, D980–D985 (2014).
62. Szpiech, Z. A. et al. Long runs of homozygosity are enriched for deleterious variation. *Am. J. Hum. Genet.* **93**, 90 (2013).
63. Sastre Moll J. Economía y sociedad en el Reino de Mallorca. Primer tercio del siglo XIV. (1987).
64. Seguí Beltrán, A. Unas islas asediadas? La defensa de las Baleares (1480–1620). *TDX (Tesis Doctorals en Xarxa)* (2018).
65. Rozenberg, D. Endogamia i problemes d'identificació a Eivissa: l'exemple de Sant Miquel. *Eivissa* **12**, 37–40 (1981). ISSN 1130–7803, ISSN-e 2385–3476, (Ejemplar dedicado a: Sa Drassana), 37–40 (1981).

Acknowledgements

We thank the volunteers who provided their samples for making this study possible. This work was supported by the Spanish Ministry of Science and Innovation (grant number PID2019-106485GB-I00) funded by the MCIN/AEI/10.13039/501100011033. We thank Inés Quintela and the National Genotyping Center (CEGEN – USC) for their assistance in genotyping the SNP arrays.

Author contributions

J.A.-I., D.C. and F.C. designed the study. J.A.-I. conducted the analysis. J.A.-I, D.C. and F.C. contributed to the interpretation of the data. J.A.-I. wrote the manuscript with help of D.C. and F.C., and E.M.-C. and M.B.-O. contributed with the sampling and helped contextualizing the results. All authors revised and approved the manuscript.

Declarations

Competing interests

The authors declare no competing interests.

Additional information

Supplementary Information The online version contains supplementary material available at https://doi.org/10.1038/s41598-024-84271-w.

Correspondence and requests for materials should be addressed to F.C.